atmosphere

MDPI

Article

Magnetic Assessment of Transplanted *Tillandsia* spp.: Biomonitors of Air Particulate Matter for High Rainfall Environments

Daniela Buitrago Posada [1,2,3], Marcos A. E. Chaparro [1,2,*] and José F. Duque-Trujillo [3]

[1] Centro de Investigaciones en Física e Ingeniería del Centro de la Provincia de Buenos Aires (CIFICEN), UNCPBA-CICPBA-CONICET, Tandil B7000GHG, Argentina
[2] Facultad de Ciencias Exactas, Universidad Nacional del Centro de la Provincia de Buenos Aires (UNCPBA), IFAS, Tandil B7000GHG, Argentina
[3] Applied Sciences School, EAFIT University, 3300 Medellín, Colombia
* Correspondence: chapator@exa.unicen.edu.ar; Tel.: +54-249-4385661

Abstract: Complementary methodologies in air quality monitoring, such as magnetic biomonitoring, are currently implemented since atmospheric particle pollution is a relevant problem for human health and ecosystems. We carried out magnetic biomonitoring using transplanted species of *Tillandsia recurvata* and *T. usneoides* to study their retention capacity of airborne magnetic particles AMP, the influence of precipitation, and magnetic properties. Plants of both epiphytic species were exposed for two, three and twelve months under uncovered and covered rain exposure conditions. The mass-specific magnetic susceptibility χ increases for both species over time, mean (s.d.) values of χ = 6.1 (6.4)–47.9 (37.6) $\times$ 10^{-8} m^3 kg^{-1}. The comparison of χ between exposure conditions suggests an insignificant rainfall influence on the accumulation/loss of magnetic particles in the studied plants. Magnetic parameters, scanning electron microscopy, and X-ray energy dispersive spectroscopy indicate the presence of magnetite and Fe-rich particles with sizes between <0.1 and 5 μm, a harmful particle category to human health. It is concluded that both species of the genus *Tillandsia* are efficient biological indicators of AMP and convenient for air particle pollution assessment in high-precipitation environments.

Keywords: air particle pollution; biological indicator; magnetic biomonitoring; magnetite; transplants

Citation: Buitrago Posada, D.; Chaparro, M.A.E.; Duque-Trujillo, J.F. Magnetic Assessment of Transplanted *Tillandsia* spp.: Biomonitors of Air Particulate Matter for High Rainfall Environments. *Atmosphere* **2023**, *14*, 213. https://doi.org/10.3390/atmos14020213

Academic Editor: Maurice Millet

Received: 8 December 2022
Revised: 16 January 2023
Accepted: 16 January 2023
Published: 19 January 2023

1. Introduction

Anthropogenic air pollution is a primary factor affecting ecosystems and human health and contributes to climate change. Pollution threatens biodiversity because sources of emission are numerous and large-scale, such as industrial activity, power-producing stations, combustion engines, and automobiles [1]. Particulate matter (PM) is one of these types of pollutant emissions. These particles are divided into three groups of interest: ultrafine (diameters less than 0.1 μm), fine (from 0.1 to 2.5 μm), and coarse (between 2.5 and 10 μm). It is known that magnetic particles are part of the components found in these groups [2]. Small aerodynamic sizes make these particles harmful by their greater capacity to lodge into the deeper part of the lungs, heart, and brain, causing respiratory and cardiovascular diseases [3], neurodegenerative diseases [4], and even cancer. In addition, air pollution increases the cost of health and has been linked to mental health [5–7].

Air quality related to PM in cities is often evaluated using sampling stations that measure the concentration of PM_{10} and $PM_{2.5}$. Stations are expensive and fixed to particular sites, limiting the sampling scope range. Therefore, alternative methods have been implemented to study atmospheric PM. Environmental magnetism, a relatively new science [8], uses magnetic parameters to investigate the presence of magnetic contaminants in the environment. One of the most valuable parameters in magnetic monitoring is the mass-specific

magnetic susceptibility (χ) used as a magnetic proxy for pollution. Magnetic biomonitoring [9], using lichens, bryophytes, tree barks and leaves, and other organisms [10–12], has proven helpful in studying air particle pollution. These biomonitors act as passive collectors and allow obtaining information about the environment quickly and at a low cost [13,14]. In this work, epiphytic plants were used, widely known organisms in studies of environmental magnetism [15–17]. Epiphytes are plants that germinate on other plants and do not have parasitic roots during all stages of their life [18]. Plants with this lifestyle can use other non-living structures as support or background to grow [18,19]. These epiphytic plants are generally long-lived perennials, and they grow relatively slowly. They obtain water and nutrients from the environment, for which many have developed morphological structures such as succulent leaves, trichomes, and spongy tissues for water absorption [20].

Two epiphytic species, i.e., *Tillandsia recurvata* and *Tillandsia usneoides*, from the Tillandsioideae subfamily, were studied in this contribution. Members of this group are characterized by their ability to obtain water and nutrients from the atmosphere, making them noticeable as an air pollution biomonitor [21]. *T. recurvata* and *T. usneoides* are native species from tropical and subtropical America [22] and are currently in the least concern conservation category. These species have been used as a biomonitor in pollution studies due to their presence in urban environments, such as metropolitan and industrial areas, which are contaminated by potentially toxic elements and other air pollutants [23–25].

The present work aims to evaluate the functionality of *T. recurvata* and *T. usneoides* in magnetic biomonitoring, assessing aspects such as the AMP accumulation record over time, the effect of precipitation on accumulation, and the inter-comparison between both species for this monitoring technique. For the latter, we study whether the capacity of *T. usneoides* as an AMP biomonitor is comparable to that of *T. recurvata*. Since the occurrence of both species varies within the study area, it would allow us to expand the space resolution by using both species for transplantation.

2. Materials and Methods

The experiments were carried out in Medellin, a tropical city with annual precipitation of around 1600 mm and an annual mean temperature of 22 °C, during the period June–October 2017 and February 2018–February 2019 at the EAFIT University campus (6°12′01.6″ N; 75°34′42.4″ W). The campus is located between two main avenues east of the Medellin river: Las Vegas Ave., with an average vehicle traffic of 439 veh h^{-1}, and Regional Ave., with an average vehicle traffic of 510 veh h^{-1} during this study [26]. This area, mainly residential, is influenced by industrial centers on the western side of the river and the metropolitan Metro train that moves along Regional Avenue (Figure 1).

The air exposure stations (AES, Figure 1a) were designed for this study using *T. recurvata* and *T. usneoides* species, as shown in Figure 1b,c. Nine AESs were located within the campus (Figure 1d). These stations correspond to wooden pillars of 1.60 m with plastic grids on both sides at the upper part, each measuring 40 × 50 cm. An acrylic plastic roof protected one of the sides (Figure 1a). The plants were harvested in a clean rural area located north of the city, 20 km from the study site, at an altitude of 1900 m.a.s.l. For *T. recurvata*, specimens of approximately 7 cm in length were taken; for *T. usneoides*, specimens of around 20 cm were taken to maintain their usual pendular growth. The exposure of the samples took place in three periods. Period 1 (P1) comprised 54 days of exposure for 36 plants (25 June to 18 August 2017). Period 2 (P2) consisted of 104 days of exposure for 36 plants (25 June to 7 October 2017). Period 3 (P3) comprised 358 days for 48 plants (13 February 2018, to 7 February 2019). In each AES, eight plants were exposed: 4 specimens of *T. recurvata* and 4 of *T. usneoides*. For each species, two specimens were installed in a covered condition (under an acrylic plastic roof, Figure 1a) and two in an uncovered condition (without a roof). Four of the eight plants were collected for P1 and four for P2 (2 per species). For Period 3, six AES (AES4 to AES9) were used, and only *T. recurvata* specimens were exposed, eight in each AES in both conditions: C and UC. The total sample size was n = 118 (only two were lost).

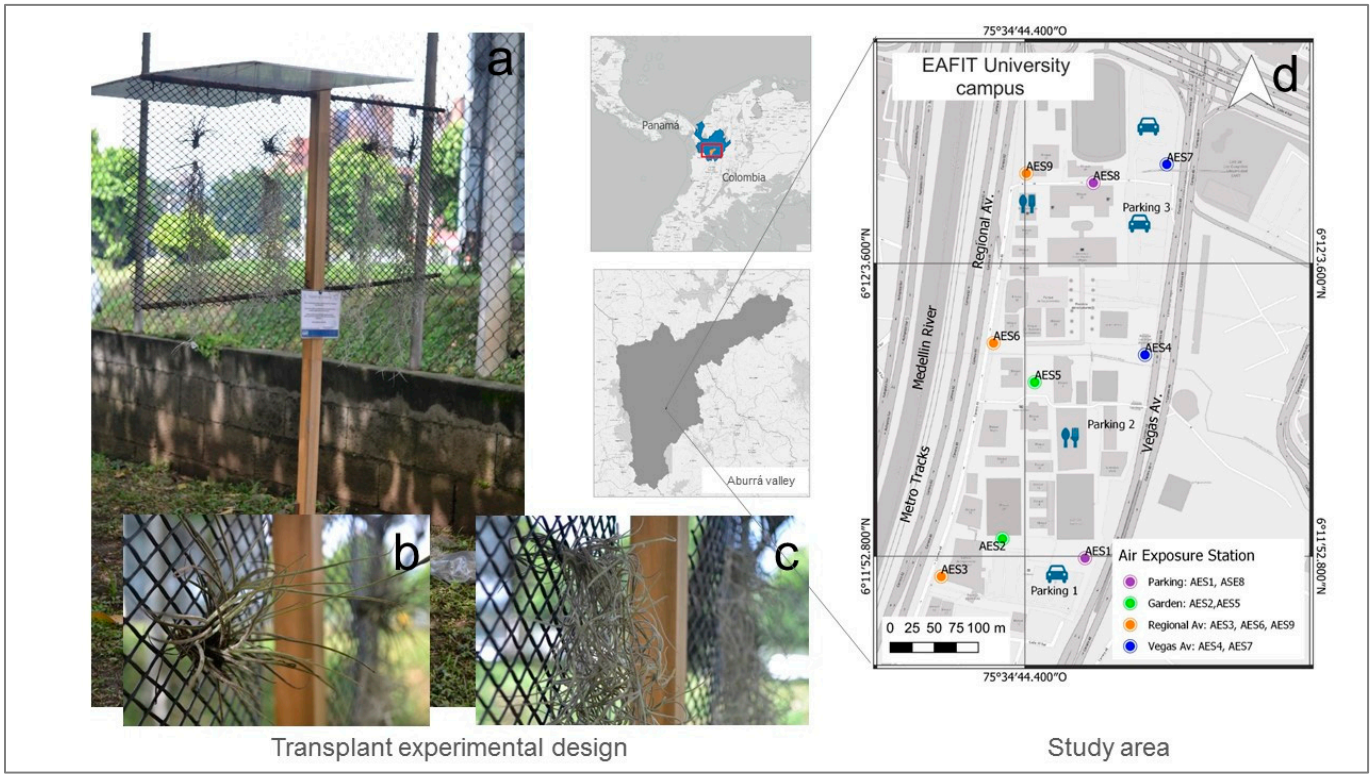

Figure 1. Experimental design: (**a**) air exposure station (AES); (**b**) *Tillandsia recurvata*; (**c**) *Tillandsia usneoides*. (**d**) Study area.

All samples were collected in paper bags and dried in an oven at 38 °C. Specimens of *T. recurvata* remained during four days of drying, while those of *T. usneoides* remained dry for five days due to their larger size. Each sample was crushed and firmly placed into 8 cm^3 plastic containers to avoid spatial reconfigurations that could cause changes in the remanent magnetization measurements.

A kappabridge MFK1 (AGICO Inc., Brno, Czech Republic) was used for magnetic susceptibility measurements, applying a field of ~200 A/m. The mass-specific magnetic susceptibility (χ) was measured in the Paleomagnetism and Environmental Magnetism Laboratory (EAFIT, Medellín, Colombia). At the Laboratory of Environmental Magnetism (UNCPBA, Tandil, Argentina), remanent magnetization measurements were carried out. The anhysteretic remanent magnetization (ARM) was imparted to all samples using a partial ARM (pARM) device coupled with an alternating field (AF) demagnetizer (Molspin Ltd., Newcastle upon Tyne, Tyne and Wear, England), superposing a DC bias field of 10, 50 and 90 μT to a peak AF of 100 mT and at an AF decay rate of 17 μT per cycle. The specific anhysteretic susceptibility (χ_{ARM}) was calculated from these ARM measurements, the anhysteretic ratio χ_{ARM}/χ, and King's plot was constructed [27]. The isothermal remanent magnetization (IRM) was determined using an ASC Scientific Pulse Magnetizer (Narragansett, RI, USA) model IM-10-30. Samples were magnetized in 27 steps by exposing each sample to increasing fields from 1.7 mT to 2470 mT. The IRM saturation (SIRM) was determined at a field of 2470 mT. The acquisition coercivity ($H_{1/2}$), remanent coercivity (H_{cr}), and S-ratio (=$-IRM_{-300\,mT}$/SIRM) were obtained by applying a reverse field once the SIRM was reached. The ARM and IRM were measured using a JR-6 spinner magnetometer (AGICO Inc., Brno, Czech Republic). Parameter χ is roughly proportional to the concentration of paramagnetic and ferrimagnetic minerals, but ARM, χ_{ARM} and SIRM are only sensitive to ferromagnetic (s.l.) minerals. Other parameters and ratios are indicative of magnetic mineralogy ($H_{1/2}$, H_{cr} and S-ratio) and magnetic grain size (χ_{ARM}/χ and ARM/SIRM) [15].

The micrographs of plants and particles were observed by scanning electron microscopy (SEM) using a PHENOM brand microscope (model G2 Pro) with 5 kV, 10 kV and 15 kV illumination at the Materials Research Laboratory EAFIT. The elemental composition of particles was determined by X-ray energy dispersive spectroscopy (EDS), carried out with a Zeiss SmartEDX coupled to the PHENOM SEM.

The Kruskal–Wallis test [28], a non-parametric one-way analysis of variance, was implemented to compare the medians of samples and determine differences at the significance level of 0.05, using Origin 8 software.

3. Results

Magnetic measurements of transplanted *T. recurvata* and *T. usneoides* exposed over the three periods and under covered and uncovered conditions are summarized in Table 1.

Table 1. Descriptive statistics of magnetic parameters for transplanted *Tillandsia* spp. over periods P1, P2 and P3.

Magnetic Parameter	n	Mean	Standard Deviation	Minimum	Median	Maximum
χ (10^{-8} m^3 kg^{-1})	118	24.6	31.2	−2.5	13.7	164.2
χ_{ARM} (10^{-8} m^3 kg^{-1})	118	47.3	47.3	6.0	31.4	285.0
ARM (10^{-6} A m^2 kg^{-1})	118	33.8	33.9	4.1	21.7	202.2
SIRM (10^{-3} A m^2 kg^{-1})	117	2.4	2.6	0.3	1.6	14.2
H_{cr} (mT)	117	36.5	3.1	27.7	37.1	53.4
S-ratio (a.u.)	117	–	–	0.68	–	1
χ_{ARM}/χ (a.u.)	114	3.8	8.4	0.1	2.0	85.6
ARM/SIRM (a.u.)	117	0.015	0.008	0.006	0.014	0.093

3.1. Magnetic Properties

The acquisition IRM measurements reach between 95% and 97% of SIRM at fields of 300 mT (Figure 2a), and most of the S-ratio values range between 0.96 and 0.98, indicating the predominance of ferrimagnetic minerals. The $H_{1/2}$ ranges between 53.4 and 67.5 mT, indicative of magnetite-like minerals [29]. In addition, the mean (s.d.) values of H_{cr} = 36.5 (3.1) mT (Table 1) confirm the presence of magnetite-like minerals.

The magnetic particle size distribution is based on anhysteretic ratios such as χ_{ARM}/χ (3.8 (8.4)), ARM/SIRM (0.015 (0.008), Table 1) and King's plot. Magnetic particles of <0.1–5 μm in size are determined for both *T. recurvata* and *T. usneoides* (Figure 2b). For P3, the sample sizes are between 1 and 5 μm. Sizes < 1 μm are only observed for periods P1 and P2.

Particle morphologies and sizes were observed by SEM, showing particles with different morphologies, from spherules to irregular particles of ~1 and 2 μm in diameter (Figure 3), which agree with estimations based on King's plot. The compositional analysis (EDS) evidences the presence of iron-rich particles; Figure 3a,b shows spherules in *T. recurvata* with variable Fe contents (37.8 to 69.9 wt%). Additionally, *T. usneoides* samples present particles with variable morphology and Fe contents from 23.7 to 47.9 wt% (Figure 3c).

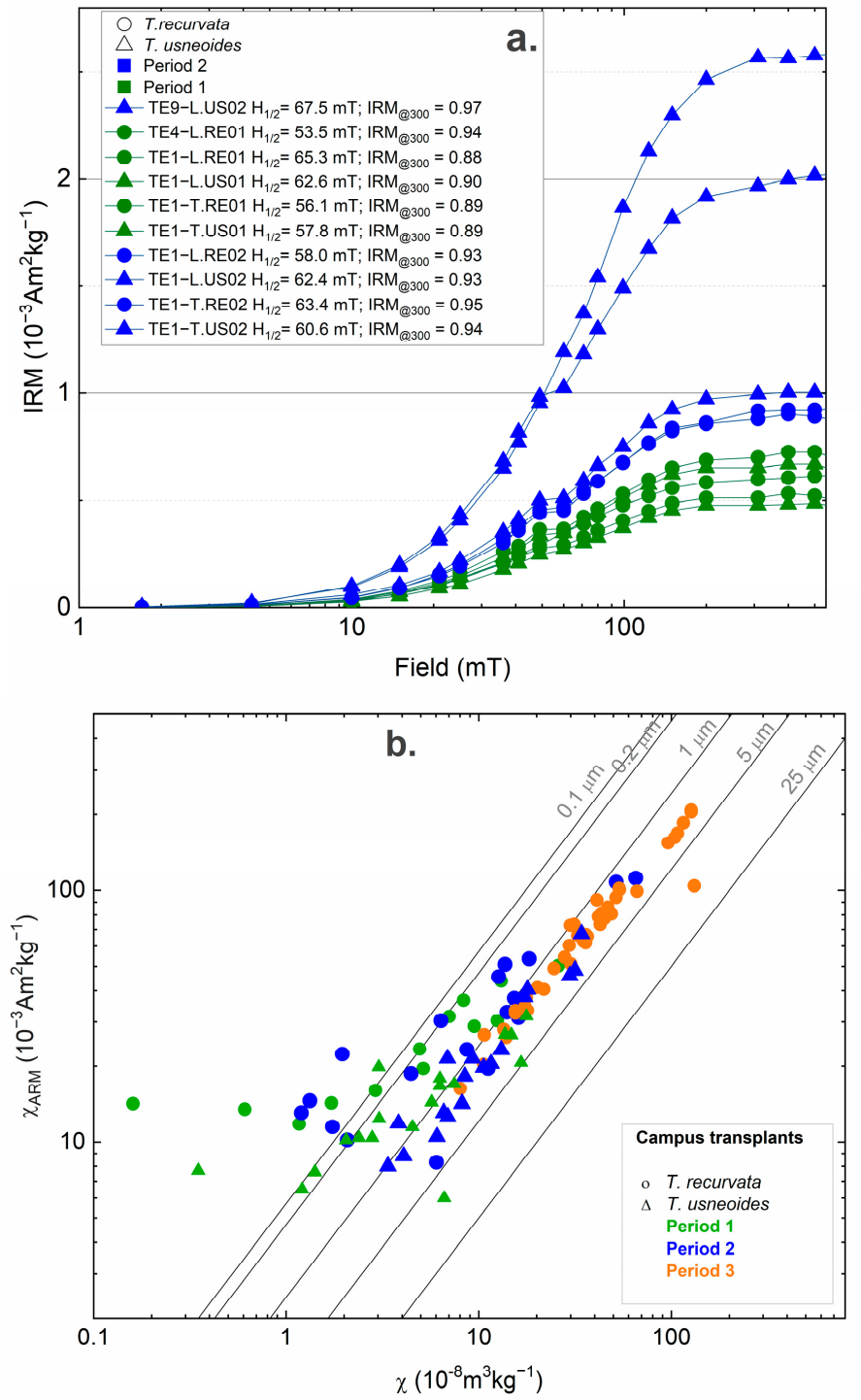

Figure 2. (**a**) Measurements of acquisition isothermal remanent magnetization for *T. recurvata* and *T. usneoides*. The IRM reaches saturation at 300 mT. The acquisition coercivity values are detailed. (**b**) Estimation of magnetic particle size for samples from every exposure period is based on the calibration lines of King's plot [27].

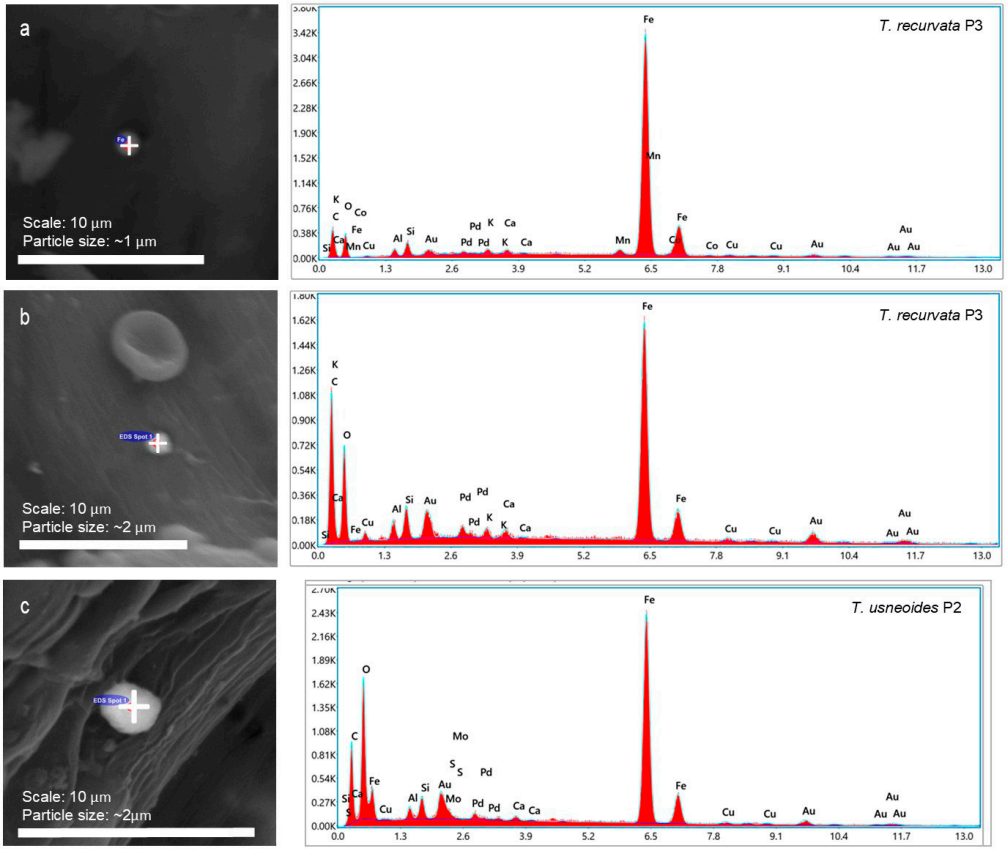

Figure 3. SEM-EDS analysis. (**a**,**b**) Spherical particles of ~1 and 2 µm in *T. recurvata* from P3. (**c**) Spherule of ~2 µm in *T. usneoides* from P2. The elemental composition of analyzed particles (cross) is shown.

3.2. Magnetic Measurements over Time

A diamagnetic signal ($\chi < 0$) was presented by control samples (Table 2) and 4 out of 118 exposed plants, as observed in Figure 4, which corresponds to specimens of *T. recurvata* from P1. The other exposed samples show positive values of χ, in agreement with ferromagnetic particles determined in Section 3.1.

Table 2. Measurements of magnetic susceptibility χ of *Tillandsia recurvata* and *Tillandsia usneoides* for exposure periods and cover (C) and uncover (UC) exposure conditions.

Exposure Condition		χ (10^{-8} m^3 kg^{-1})									
		T. recurvata					*T. usneoides*				
		n	**Median**	**Mean (s.d.)**	**Min–Max**	**Increase (of Mean)**	***n***	**Median**	**Mean (s.d.)**	**Min–Max**	**Increase (of Mean)**
Control	–	21	−5.1	−5.8 (3.9)	−13.3–0.0	0					
P1	C	9	1.2	4.8 (6.2)	−0.7–15.9	1.8	9	4.5	5.9 (5.1)	0.4–14.8	2.0
	UC	9	4.9	6.9 (8.7)	−2.5–25.9	2.2	9	6.3	7.0 (6.2)	1.2–17.7	2.2
P2	C	9	8.7	13.0 (15.8)	1.3–51.8	3.2	9	8.5	12.7 (9.5)	3.8–34.2	3.2
	UC	9	12.7	15.0 (19.6)	1.2–65.4	3.6	9	9.3	12.8 (10.5)	3.4–31.6	3.2
P3	C	22	45.9	48.5 (33.5)	10.6–126.9	9.4	–	–	–	–	–
	UC	24	32.9	47.4 (41.8)	8.0–164.2	9.2	–	–	–	–	–

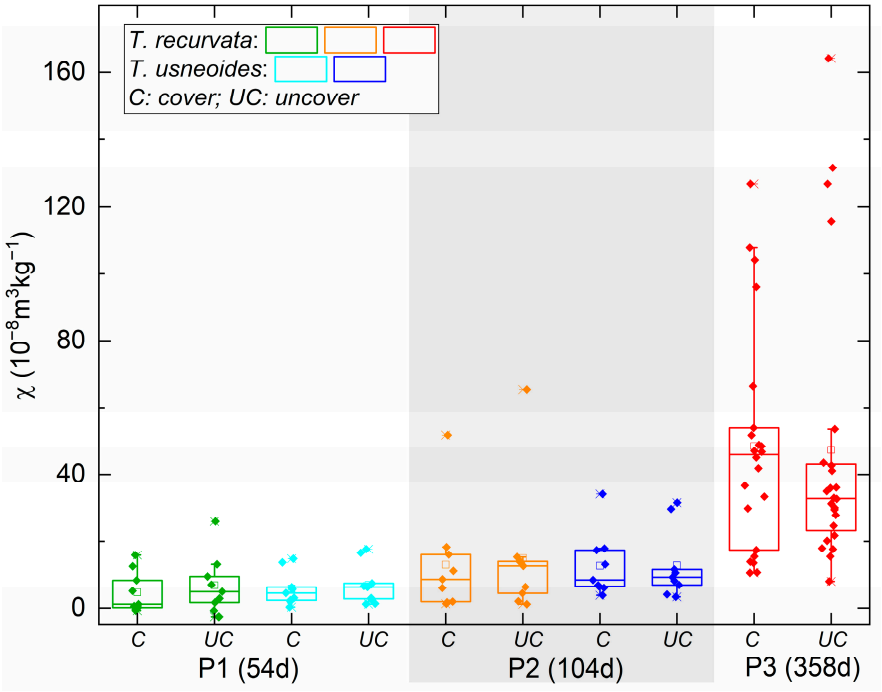

Figure 4. Mass-specific magnetic susceptibility for transplants of *T. recurvata* and *T. usneoides*. P1 (54 days of exposure); P2 (104 days of exposure); P3 (358 days of exposure).

During the three exposure periods, an increase in time for magnetic susceptibility is observed for all samples along the experiment (Figure 4). In particular, the mean (s.d.) values of χ for periods increase from $\chi = -5.8$ (3.9), 6.1 (6.4) to 13.4 (13.9) and 47.9 (37.6) $\times 10^{-8}$ m^3 kg^{-1} for unexposed samples (control), P1, P2, and P3, respectively, evidencing the accumulation of AMP over time for both biomonitors (Table S1, Supplementary Material). The eight highest values of χ (>90 $\times 10^{-8}$ m^3 kg^{-1}, Figure 4) were measured in P3 and correspond to the same exposure site, AES9 (see Figure 1d). Moreover, the highest values observed for P2 belong to the same site.

The covered and uncovered exposure conditions show that both species in P1 and P2 have similar χ values, i.e., χ values for uncovered are equal to or higher than the values for the covered condition (Table 2). In P3, there is a partial decrease of χ for plants exposed in the uncovered (χ = 47.4 (41.8) $\times 10^{-8}$ m^3 kg^{-1}) compared to the covered condition (χ = 48.5 (33.5) $\times 10^{-8}$ m^3 kg^{-1}, Table 2). However, the highest values ($\chi > 90 \times 10^{-8}$ m^3 kg^{-1}) were recorded in samples under both conditions (Figure 4, P3). Generally, there is a minimal difference between the two exposure conditions, which is notable in the mean values for each treatment or condition.

Figure S1 (Supplementary Material) shows rainfall recorded for Medellin [30] during the experimental periods. A characteristic bimodal rainfall annual pattern is observed. Even with rainfall events, plants increase their magnetic susceptibility. P3 covered the annual rainfall cycle of 2018 (annual rainfall is 2030 mm for 2018), where both transplanted species showed the highest χ values.

Both studied species, *T. recurvata* and *T. usneoides*, present an increase of χ over time, which was higher in *T. usneoides* (mean (s.d.) values of χ = 6.4 (5.5) $\times 10^{-8}$ m^3 kg^{-1}) than in *T. recurvata* (χ = 5.8 (7.4) $\times 10^{-8}$ m^3 kg^{-1}) for P1, but for P2, the opposite was observed (Table S2, Supplementary Material).

4. Discussion

4.1. Magnetic Particle Accumulation on Tillandsia spp.

Biological tissues of epiphytic plants present a diamagnetic signal where the χ value is negative. Although only four transplants of *T. recurvata* have a negative χ value be-

cause they trapped insignificant AMP over P1; the magnetic signal of exposed plants (e.g., χ = 24.6 (31.2) $\times$ 10^{-8} m^3 kg^{-1}; Table 1) shows variable contents of accumulated AMP in these organic tissues.

Particle size estimations (<0.1–5 µm) and SEM-EDS confirm that accumulated Fe-rich particles are typically related to anthropogenic sources (Figures 2b and 3). It is noticed that the shiny particles have a spherical morphology, commonly reported as the anthropogenic origin from vehicular and industrial sources [21,31,32]. These particle sizes, especially those smaller than 2.5 µm, are the most harmful to human health because they can reach deeper into the lungs and vital human organs [4].

Studied transplants of *Tillandsia* spp. were able to trap this type of harmful AMP. Moreover, these results agree with particle sizes (2–5 µm) reported by [33], who carried out extensive magnetic biomonitoring using native individuals of *T. recurvata* in the Aburrá Valley.

The magnetic mineralogy (IRM, H_{cr}, and $H_{1/2}$ coercivity parameters) reveals the predominance of magnetite. Figure 5 shows similarities between H_{cr} values for this study and reported values for industrial, residential, and vehicular areas from Aburrá Valley [33]. The statistical comparison between χ medians for transplants (EAFIT University campus, this study) and native species of the industrial and vehicular areas from Aburrá Valley gives no significant differences at the 0.05 level (Table S3, Supplementary Material). This fact proves that accumulated AMP by transplants in a specific location (EAFIT University campus) have a common origin with extensive areas affected by industries and vehicular traffic. Although both pollutant types are present in Medellín, the primary source appears to have a characteristic magnetic signature associated with traffic emissions [14,34,35].

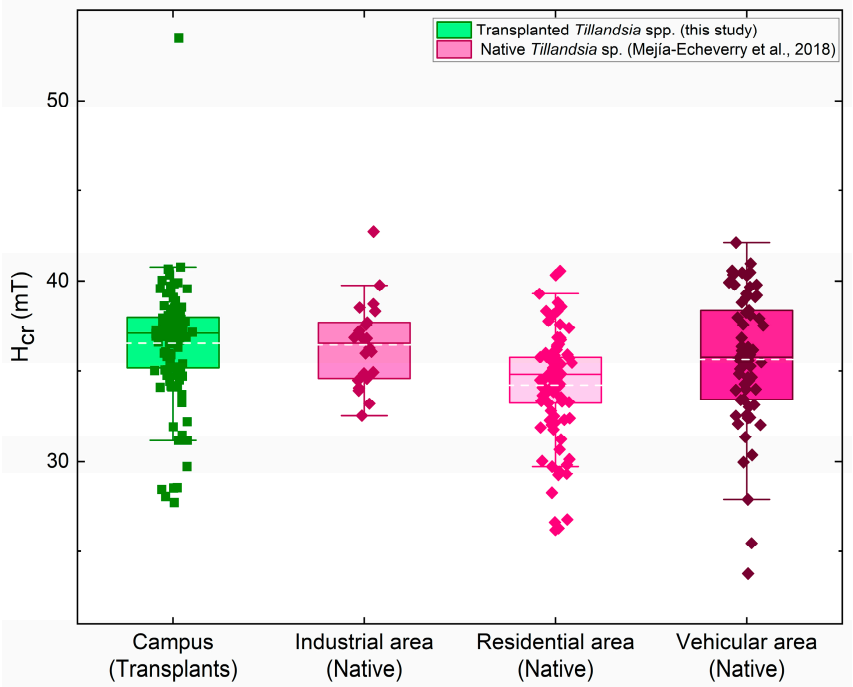

Figure 5. Comparison of H_{cr} between transplanted (Campus, this study) and native *Tillandsia* spp. [33]. The box delineates the interquartile range of 25–75% (Q1–Q3), and horizontal lines in the box indicate the mean (dash) and median (solid). The minimum and maximum values are shown using whiskers.

4.2. Exposure Periods, Rainfall Influence and Comparison between Species

It is evident that the longer the exposure time, the higher the χ acquired by transplanted species. The median values of χ, i.e., AMP accumulation, are significantly different at the 0.05 level between periods (Table S4, Supplementary Material). After about two months, both species reach mean (s.d.) values of χ = 6.1 (6.4) $\times$ 10^{-8} m^3 kg^{-1}. Moreover, χ values increase about two, three, and nine-fold over two, three, and twelve months from

unexposed samples, P1, P2, to P3, respectively (Figure 4, Table S1, Supplementary Material). Outlier values represent the highest χ recorded for some transplants related to site AES9, located 30 m from Regional Avenue. The contribution of AMP in this site seems to be the most important because it has high traffic flow (average vehicular intensity of 493 veh h^{-1} for P1-P2 and 422 veh h^{-1} for P3 [26]) with regular freight truck transit, including the metropolitan metro train at a distance of 50 m (Figure 1). Other stations associated with Regional Ave. (e.g., χ = 25.6 (16,2) × 10^{-8} m^3 kg^{-1}, AES6), Las Vegas Ave. (e.g., χ = 23.6 (17.3) × 10^{-8} m^3 kg^{-1}, AES7) and a parking site (e.g., χ = 24.7 (22.3) × 10^{-8} m^3 kg^{-1}, AES8) show a higher χ in contrast to the stations located in the internal campus gardens (χ = 3.6 (4.2), AES2; χ = 10.0 (8.2) × 10^{-8} m^3 kg^{-1}, AES5; Table S5, Supplementary Material). This fact indicates that the locations of this transplanted species effectively offer AMP pollution information about a specific site, allowing it to carry out a comparative framework with other sampling sites to provide a pollution assessment of a selected area.

At the time of sample collection, in site AES9, dark dust was visible on the leaves. It is known that plants suffer morphological and physiological damage from various pollutants. Specifically, it has been reported that the deposition of particulate matter on the leaf surface generates a shading effect and can obstruct the stomata, which results in a decrease in chlorophyll concentration affecting photosynthetic processes and protein synthesis, making the plant more vulnerable to pathogens [36–38]. In addition, transplanted individuals are more susceptible to damage due to stress caused by handling and relocation.

The highest magnetic susceptibility value recorded in transplants is 164.0 × 10^{-8} m^3 kg^{-1} for about one-year exposure time (358 days), which is lower than values reported for native *T. recurvata* in Aburrá Valley (χ = 372.9 × 10^{-8} m^3 kg^{-1} for a vehicular zone [33]. Present data suggest that transplanted species do not reach AMP saturation over a long exposure period of one year. It is difficult to standardize the accumulation time of native epiphytic plants because their growth rate is not precise and varies depending on the availability of water, CO_2, and handy nutrients [39]. The size of each plant is determined by its age and phenotypic plasticity, the ability of organisms to change their observable characters according to environmental variables under which they develop. Variables such as humidity, radiation, temperature, and water availability can frequently change in an urban habitat such as the one colonized by the *Tillandsia* spp., and even in vascular epiphytes, which could have a more pronounced impact on their size [40,41]. For these reasons, transplants appear essential for AMP biomonitoring since the exposition time is known.

Rainfall events are a notable meteorological factor for magnetic biomonitoring; hence, it is essential to evaluate this issue in one of the rainiest countries in the world. For Aburrá Valley, a rainfall of 2381 mm was recorded during the three exposition periods, i.e., 200 mm, 411 mm, and 1970 mm for P1, P2, and P3, respectively. This indicates that even with rainfall events, transplanted *Tillandsia* spp. increase their magnetic susceptibility significantly. Precipitation is a factor that can influence biomonitor function. It has been reported that climatic aspects, such as precipitation and wind, can remove, wash or leach particulate matter accumulated by plant leaves used as biomonitors [42,43]. During the present study, different exposure conditions (i.e., covered and uncovered) were implemented to investigate the precipitation effect on transplanted individuals. The comparison between χ medians for each period, exposure conditions, and species give no significant differences at the 0.05 level (Table S6, Supplementary Material).

Uncovered plants were expected to report lower magnetic susceptibility values than covered ones because rain could fall directly over uncovered leaves and wash out the accumulated particles. Although the χ values for uncovered plants are slightly higher than the covered plants (Table 2), such differences are insignificant (Table S6, Supplementary Material). These results provide evidence that exposition to rain generates insignificant differences between the χ values for both conditions and species *T. recurvata* and *T. usneoides*. Moreover, such minor differences are observed over monthly and annual periods where rainfall varied from 200 mm to 1970 mm. It is found that precipitation seems to have a minimal effect on the accumulation and loss of AMP in these *Tillandsia* species.

In biomonitoring, the morphology and surface properties of tree leaves are used to determine the capacity for particle retention [44,45]. In addition, the surface of the sheets with high roughness and wettability has a strong retention ability; more roughness results in a stronger retention capacity, which is related to the amount of retained particles [46,47]. However, it is worth mentioning that leaves from these epiphytic species have distinctive characteristics from tree leaves. They have a unique foliar trichome system, where trichome wings are elevated or folded and stuck to the leaf surface during low- or high-moisture conditions, respectively. This flattening of the trichomes on the leaves of *Tillandsia* caused a marked reduction in the contact angles resulting in liquid spreading over the surface of *Tillandsia* leaves [48]. Thus, the low influence of precipitation for *T. recurvata* and *T. usneoides* may be caused by the particular characteristics of these leaves.

SEM images (Figure 6) show that trichomes cover the leaves entirely in both plants. Trichomes for *T. usneoides* (with a smooth edge) are around 600 µm in length, which is longer than for *T. recurvata* (about 150 µm). It is possible that the water droplets displace the coarser particles between the trichomes but do not remove them altogether; hence, particles remain on the plant. It is even possible that the water droplets do not enter between the trichomes due to the pivot mechanism of trichome wings.

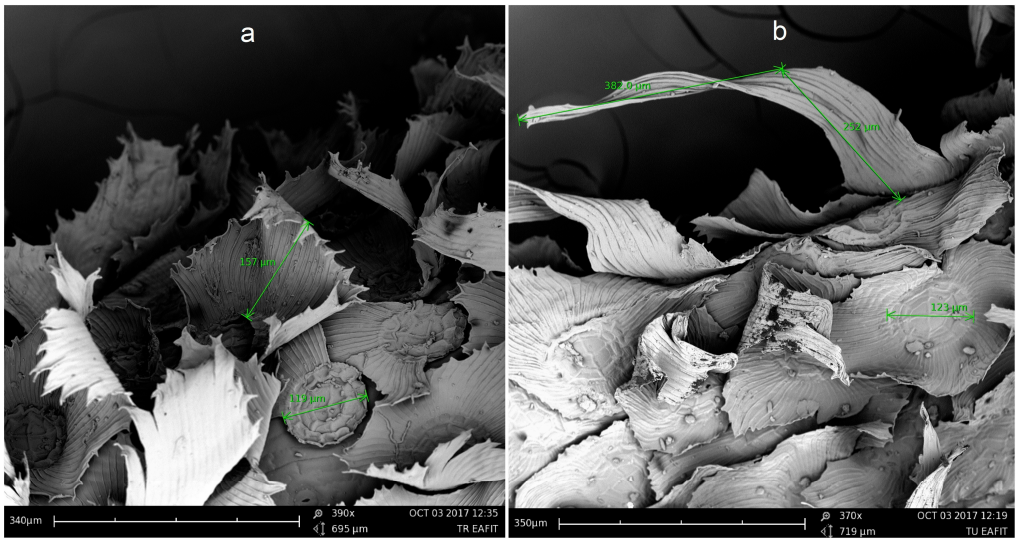

Figure 6. SEM images of *Tillandsia recurvata* (**a**) and *Tillandsia usneoides* (**b**).

Despite their different characteristics, both species showed AMP accumulation over time, thus demonstrating their functionality as an AMP biomonitor. This result has been reported for *T. recurvata* in [15,21,33] and is here reported for other species (*T. usneoides*), which have been widely used as a biomonitor to evaluate other different pollutants [24,25,49–55]. The AMP accumulation capacity of *T. usneoides* is comparable to the previously studied *T. recurvata*, which is concluded in this study through magnetic susceptibility measurements. The χ median values between both species at P1 and P2 are not significantly different at the 0.05 level (Table S6, Supplementary Material).

This similar AMP accumulation capacity of *Tillandsia* species is an essential attribute for the extrapolation of this work to other areas with high rainfall regimes, where the distribution of these species is not uniform throughout the study area. Moreover, the sampling ranges for magnetic biomonitoring using native individuals could be extended using the availability of one species in the absence of the other.

5. Conclusions

Precipitation does not significantly influence the accumulation of airborne magnetic particles in the studied *Tillandsia* species. It is possible that water only moves particulate material between the trichomes but does not wash it off entirely due to the unique trichome system

on the leaves. The exposition time can be chosen for magnetic biomonitoring experiments using transplants of *Tillandsia* species; therefore, it is an operational methodology for assessing AMP over time in high-rainfall areas. Both *Tillandsia* species trapped incremental contents of AMP for exposure periods of two (mean (s.d.) values of χ = 6.1 (6.4) $\times$ 10^{-8} m^3 kg^{-1}), three (13.4 (13.9) $\times$ 10^{-8} m^3 kg^{-1}) and twelve (47.9 (37.6) $\times$ 10^{-8} m^3 kg^{-1}) months. These efficient biomonitors increased their χ values about two, three, and nine-fold over two, three and twelve months, respectively.

Accumulated airborne particles comprise magnetite of <0.1–5 µm in size. Such harmful Fe-rich particles are related to sources of anthropogenic origin in Aburrá Valley, such as vehicular and industrial emissions. Magnetic results confirm that *Tillandsia usneoides* can accumulate these AMP in its tissues, as has been demonstrated for *Tillandsia recurvata*. The evaluation of the *Tillandsia usneoides* as a magnetic biomonitor represents the possibility of expanding the sampling range for magnetic biomonitoring in the Aburrá Valley and other heavily rainy cities, where the predominance of *T. recurvata* and *T. usneoides* varies due to environmental conditions, even in rural areas where traditional air quality monitoring systems do not exist. Thus, *T. usneoides* sp. has to be considered as another biomonitor of air particle quality for areas with high rainfall regimes.

It is necessary to emphasize the questions raised in this work regarding more extensive sampling and extended exposition periods. Furthermore, investigating some biological aspects of the studied species would provide valuable information for AMP biomonitoring.

Supplementary Materials: The following supporting information can be downloaded at: https://www.mdpi.com/article/10.3390/atmos14020213/s1, Figure S1: Monthly rainfall during exposure periods. Data were provided by IDEAM [30]. Rainfalls of 200 mm, 411 mm, and 1970 mm were recorded for periods P1, P2, and P3, respectively. Annual rainfall was 1864 and 2030 mm for 2017 and 2018, respectively; Table S1: Measurements of magnetic susceptibility χ of *Tillandsia recurvata* and *Tillandsia usneoides* for the exposure periods. Cover (C) and uncover (UC) exposure conditions; Table S2: Magnetic susceptibility χ for species *Tillandsia recurvata* and *Tillandsia usneoides*. Cover (C) and uncover (UC) exposure conditions; Table S3: Descriptive statistics and Kruskal–Wallis test for transplanted samples (Campus, this study) and native samples (Industrial, Residential and Vehicular, [33]). Statistical differences in median values of H_{cr} are indicated. YES indicates that differences are significant at the 0.05 level; Table S4: Kruskal–Wallis test for transplanted samples exposed over periods P1, P2, and P3. Statistical differences in median values of χ are indicated. YES indicates that differences are significant at the 0.05 level; Table S5: Description of the study zones and magnetic susceptibility χ of transplants for each Air Exposure Station; Table S6: Kruskal–Wallis test for transplanted species exposed over periods P1, P2, and P3. Statistical differences in median values of χ are indicated. YES indicates that differences are significant at the 0.05 level. Cover (C) and uncover (UC) exposure conditions; T.r: *Tillandsia recurvata*; T.u: *Tillandsia usneoides*.

Author Contributions: Conceptualization, M.A.E.C. and J.F.D.-T.; Formal analysis, M.A.E.C.; Funding acquisition, M.A.E.C. and J.F.D.-T.; Investigation, D.B.P. and M.A.E.C.; Methodology, D.B.P.; Visualization, M.A.E.C.; Writing—original draft, D.B.P.; Writing—review and editing, M.A.E.C. and J.F.D.-T. All authors have read and agreed to the published version of the manuscript.

Funding: This research was funded by the Universidad EAFIT and partially by the CONICET, grant number: P-UE-2017-22920170100004CO. The APC was funded by the MDPI Editorial Team.

Institutional Review Board Statement: Not applicable.

Informed Consent Statement: Not applicable.

Data Availability Statement: Not applicable.

Acknowledgments: The authors thank the Universidad EAFIT, the Universidad Nacional del Centro de la Provincia de Buenos Aires (UNCPBA), and the National Council for Scientific and Technological Research (CONICET) for their financial support. The author thanks Herica Y. Montoya for her help in the SEM analysis and the editors, Hana Grison, and anonymous reviewers whose comments improved the manuscript.

Conflicts of Interest: The authors declare no conflict of interest.

References

1. Manisalidis, I.; Stavropoulou, E.; Stavropoulos, A.; Bezirtzoglou, E. Environmental and Health Impacts of Air Pollution: A Review. *Front. Public Health* **2020**, *8*, 14. [CrossRef]
2. Chaparro, M.A.E. *Estudio de Parámetros Magnéticos de Distintos Ambientes Relativamente Contaminados En Argentina y Antártida*, 1st ed.; Geofísica UNAM: Mexico City, Mexico, 2006; p. 107. ISBN 970323567-0.
3. Calderón-Garcidueñas, L.; González-Maciel, A.; Mukherjee, P.S.; Reynoso-Robles, R.; Pérez-Guillé, B.; Gayosso-Chávez, C.; Torres-Jardón, R.; Cross, J.V.; Ahmed, I.A.M.; Karloukovski, V.V.; et al. Combustion- and Friction-Derived Magnetic Air Pollution Nanoparticles in Human Hearts. *Environ. Res.* **2019**, *176*, 108567. [CrossRef]
4. Maher, B.A.; Ahmed, I.A.M.; Karloukovski, V.; MacLaren, D.A.; Foulds, P.G.; Allsop, D.; Mann, D.M.A.; Torres-Jardón, R.; Calderon-Garciduenas, L. Magnetite Pollution Nanoparticles in the Human Brain. *Proc. Natl. Acad. Sci. USA* **2016**, *113*, 10797–10801. [CrossRef]
5. He, C.; Qiu, K.; Pott, R. Reduction of Urban Traffic–Related Particulate Matter—Leaf Trait Matters. *Environ. Sci. Pollut. Res.* **2020**, *27*, 5825–5844. [CrossRef]
6. Li, X.; Jin, L.; Kan, H. Air Pollution: A Global Problem Needs Local Fixes. *Nature* **2019**, *570*, 437–439. [CrossRef]
7. Wang, R.; Xue, D.; Liu, Y.; Liu, P.; Chen, H. The Relationship between Air Pollution and Depression in China: Is Neighbourhood Social Capital Protective? *Int. J. Environ. Res. Public Health* **2018**, *15*, 1160. [CrossRef]
8. Gribov, S.K.; Shcherbakov, V.P.; Aphinogenova, N.A. Magnetic Properties of Artificial CRM Created on Titanomagnetite-Bearing Oceanic Basalts. In *Recent Advances in Environmental Magnetism and Paleomagnetism, Proceedings of the International Conference on Geomagnetism, Paleomagnetism and Rock Magnetism, Kazan, Russia, October 2017*; Nurgaliev, D., Shcherbakov, V., Kosterov, A., Spassov, S., Eds.; Springer International Publishing: Cham, Switzerland, 2019; pp. 501–511. [CrossRef]
9. Chaparro, M.A.E. Airborne Particle Accumulation and Loss in Pollution-Tolerant Lichens and Its Magnetic Quantification. *Environ. Pollut.* **2021**, *288*, 117807. [CrossRef]
10. Brunialti, G.; Frati, L.; Carrillo, W.; Calva, J.; Benítez, Á. The Use of Bryophytes, Lichens and Bromeliads for Evaluating Air and Water Pollution in an Andean City. *Forests* **2022**, *13*, 1607. [CrossRef]
11. Leite, A.d.S.; Rousse, S.; Léon, J.F.; Trindade, R.I.F.; Haoues-Jouve, S.; Carvallo, C.; Dias-Alves, M.; Proietti, A.; Nardin, E.; Macouin, M. Barking up the Right Tree: Using Tree Bark to Track Airborne Particles in School Environment and Link Science to Society. *GeoHealth* **2022**, *6*, e2022GH000633. [CrossRef]
12. Préndez, M.; Carvallo, C.; Godoy, N.; Egas, C.; Aguilar Reyes, B.O.; Calzolai, G.; Fuentealba, R.; Lucarelli, F.; Nava, S. Magnetic and Elemental Characterization of the Particulate Matter Deposited on Leaves of Urban Trees in Santiago, Chile. *Environ. Geochem. Health* **2022**, *3*, 1–15. [CrossRef]
13. Mitchell, R.; Maher, B.A.; Kinnersley, R. Rates of Particulate Pollution Deposition onto Leaf Surfaces: Temporal and Inter-Species Magnetic Analyses. *Environ. Pollut.* **2010**, *158*, 1472–1478. [CrossRef]
14. Chaparro, M.A.E.; Chaparro, M.A.E.; Castañeda Miranda, A.G.; Marié, D.C.; Gargiulo, J.D.; Lavornia, J.M.; Natal, M.; Böhnel, H.N. Fine Air Pollution Particles Trapped by Street Tree Barks: In Situ Magnetic Biomonitoring. *Environ. Pollut.* **2020**, *266*, 115229. [CrossRef]
15. Chaparro, A.E.; M.A.E.; Chaparro, M.A.E.; Castañeda Miranda, A.G.; Böhnel, H.N.; Sinito, A.M. An Interval Fuzzy Model for Magnetic Biomonitoring Using the Specie *Tillandsia recurvata* L. *Ecol. Indic.* **2015**, *54*, 238–245. [CrossRef]
16. de la Cruz, A.R.H.; Ayuque, R.F.O.; de la Cruz, R.W.H.; López-Gonzales, J.L.; Gioda, A. Air Quality Biomonitoring of Trace Elements in the Metropolitan Area of Huancayo, Peru Using Transplanted Tillandsia Capillaris as a Biomonitor. *An. Acad. Bras. Cienc.* **2020**, *92*, 20180813. [CrossRef]
17. Morera-Gómez, Y.; Alonso-Hernández, C.M.; Armas-Camejo, A.; Viera-Ribot, O.; Morales, M.C.; Alejo, D.; Elustondo, D.; Lasheras, E.; Santamaría, J.M. Pollution Monitoring in Two Urban Areas of Cuba by Using *Tillandsia recurvata* (L.) L. and Top Soil Samples: Spatial Distribution and Sources. *Ecol. Indic.* **2021**, *126*, 107667. [CrossRef]
18. Zotz, G. *Plants on Plants—The Biology of Vascular Epiphytes*; Springer International Publishing: Cham, Switzerland, 2016. [CrossRef]
19. Wester, S.; Zotz, G. Growth and Survival of Tillandsia Flexuosa on Electrical Cables in Panama. *J. Trop. Ecol.* **2010**, *26*, 123–126. [CrossRef]
20. Benzing, D.H. *Vascular Epiphytes: General Biology and Related Biota*; Cambridge Tropical Biology Series; Cambridge University Press: Cambridge, UK, 1990; p. 354. [CrossRef]
21. Castañeda Miranda, A.G.; Chaparro, M.A.E.; Chaparro, M.A.E.; Böhnel, H.N. Magnetic Properties of *Tillandsia recurvata* L. and Its Use for Biomonitoring a Mexican Metropolitan Area. *Ecol. Indic.* **2016**, *60*, 125–136. [CrossRef]
22. Betancur Betancur, J.; Universidad Nacional deColombia. Guía de Campo: Santa María, Pintada de Flores. In *St. María, Pint. Flores*; Instituto de Ciencias Naturales Universidad Nacional de Colombia: Bogotá, Colombia, 2007; p. 172.
23. de Souza Pereira, M.; Heitmann, D.; Reifenhäuser, W.; Meire, R.O.; Santos, L.S.; Torres, J.P.M.; Malm, O.; Körner, W. Persistent Organic Pollutants in Atmospheric Deposition and Biomonitoring with *Tillandsia usneoides* (L.) in an Industrialized Area in Rio de Janeiro State, Southeast Brazil—Part II: PCB and PAH. *Chemosphere* **2007**, *67*, 1736–1745. [CrossRef]
24. Filho, G.M.A.; Andrade, L.R.; Farina, M.; Malm, O. Hg Localisation in *Tillandsia usneoides* L. (Bromeliaceae), an Atmospheric Biomonitor. *Atmos. Environ.* **2002**, *36*, 881–887. [CrossRef]
25. Markert, B. Determination of Trace Elements in Tillandsia Usneoides by Neutron Activation Analysis for Environmental Biomonitoring. *J. Radioanal. Nucl. Chem.* **2001**, *249*, 391–395. [CrossRef]

26. Secretaría de Movilidad de Medellín SIMM Sistema Inteligente de Movilidad de Medellín. Available online: https://www.medellin.gov.co/movilidad/observatorio/indicadores#2-velocidad-e-intensidad-promedio-en-los-principales-corredores-viales (accessed on 1 December 2022).
27. King, J.; Banerjee, S.K.; Marvin, J.; Özdemir, Ö. A Comparison of Different Magnetic Methods for Determining the Relative Grain Size of Magnetite in Natural Materials: Some Results from Lake Sediments. *Earth Planet. Sci. Lett.* **1982**, *59*, 404–419. [CrossRef]
28. Conover, W.J. *Practical Nonparametric Statistics*, 3rd ed.; John Wiley & Sons Inc.: New York, NY, USA, 1999; p. 608.
29. Peters, C.; Dekkers, M.J. Selected Room Temperature Magnetic Parameters as a Function of Mineralogy, Concentration and Grain Size. *Phys. Chem. Earth* **2003**, *28*, 659–667. [CrossRef]
30. IDEAM Instituto de Hidrología, Meteorología y Estudios Ambientales. Available online: http://institucional.ideam.gov.co/precipitacionTipos/precipitacionTipos.html (accessed on 1 October 2020).
31. Marié, D.C.; Chaparro, M.A.E.; Irurzun, M.A.; Lavornia, J.M.; Marinelli, C.; Cepeda, R.; Böhnel, H.N.; Castañeda Miranda, A.G.; Sinito, A.M. Magnetic Mapping of Air Pollution in Tandil City (Argentina) Using the Lichen Parmotrema Pilosum as Biomonitor. *Atmos. Pollut. Res.* **2016**, *7*, 513–520. [CrossRef]
32. Chaparro, M.A.E.; Lavornia, J.M.; Chaparro, M.A.E.; Sinito, A.M. Biomonitors of Urban Air Pollution: Magnetic Studies and SEM Observations of Corticolous Foliose and Microfoliose Lichens and Their Suitability for Magnetic Monitoring. Environmental Pollution. 2013;1. *Environ. Pollut.* **2013**, *172*, 61–69. [CrossRef] [PubMed]
33. Mejía-Echeverry, D.; Chaparro, M.A.E.; Duque-Trujillo, J.F.; Chaparro, M.A.E.; Castañeda Miranda, A.G. Magnetic Biomonitoring as a Tool for Assessment of Air Pollution Patterns in a Tropical Valley Using *Tillandsia* Sp. *Atmosphere* **2018**, *9*, 283. [CrossRef]
34. Sagnotti, L.; Taddeucci, J.; Winkler, A.; Cavallo, A. Compositional, Morphological, and Hysteresis Characterization of Magnetic Airborne Particulate Matter in Rome, Italy. *Geochem. Geophys. Geosystems* **2009**, *10*. [CrossRef]
35. Winkler, A.; Contardo, T.; Vannini, A.; Sorbo, S.; Basile, A.; Loppi, S. Magnetic Emissions from Brake Wear Are the Major Source of Airborne Particulate Matter Bioaccumulated by Lichens Exposed in Milan (Italy). *Appl. Sci.* **2020**, *10*, 2073. [CrossRef]
36. Fusaro, L.; Salvatori, E.; Winkler, A.; Frezzini, M.A.; De Santis, E.; Sagnotti, L.; Canepari, S.; Manes, F. Urban Trees for Biomonitoring Atmospheric Particulate Matter: An Integrated Approach Combining Plant Functional Traits, Magnetic and Chemical Properties. *Ecol. Indic.* **2021**, *126*, 107707. [CrossRef]
37. Rai, P.K. Impacts of Particulate Matter Pollution on Plants: Implications for Environmental Biomonitoring. *Ecotoxicol. Environ. Saf.* **2016**, *129*, 120–136. [CrossRef]
38. Joshi, P.; Swami, A. Air Pollution Induced Changes in the Photosynthetic Pigments of Selected Plant Species. *J. Environ. Biol.* **2009**, *30*, 295–298.
39. Zotz, G.; Bogusch, W.; Hietz, P.; Ketteler, N. Growth of Epiphytic Bromeliads in a Changing World: The Effects of CO2, Water and Nutrient Supply. *Acta Oecologica* **2010**, *36*, 659–665. [CrossRef]
40. Zotz, G. Size-Related Intraspecific Variability in Physiological Traits of Vascular Epiphytes and Its Importance for Plant Physiological Ecology. *Perspect. Plant Ecol. Evol. Syst.* **2000**, *3*, 19–28. [CrossRef]
41. de la Rosa-Manzano, E.; Andrade, J.L.; Zotz, G.; Reyes-García, C. Physiological Plasticity of Epiphytic Orchids from Two Contrasting Tropical Dry Forests. *Acta Oecologica* **2017**, *85*, 25–32. [CrossRef]
42. Zhang, R.; Ma, K. The Impact of Climate Factors on Airborne Particulate Matter Removal by Plants. *J. Clean. Prod.* **2021**, *310*, 127559. [CrossRef]
43. Zhou, S.; Cong, L.; Liu, Y.; Xie, L.; Zhao, S.; Zhang, Z. Rainfall Intensity Plays an Important Role in the Removal of PM from the Leaf Surfaces. *Ecol. Indic.* **2021**, *128*, 107778. [CrossRef]
44. Chávez-García, E.; González-Méndez, B. Particulate Matter and Foliar Retention: Current Knowledge and Implications for Urban Greening. *Air Qual. Atmos. Health* **2021**, *14*, 1433–1454. [CrossRef]
45. Liu, J.; Cao, Z.; Zou, S.; Liu, H.; Hai, X.; Wang, S.; Duan, J.; Xi, B.; Yan, G.; Zhang, S.; et al. An Investigation of the Leaf Retention Capacity, Efficiency and Mechanism for Atmospheric Particulate Matter of Five Greening Tree Species in Beijing, China. *Sci. Total Environ.* **2018**, *616–617*, 417–426. [CrossRef]
46. Li, X.; Zhang, T.; Sun, F.; Song, X.; Zhang, Y.; Huang, F.; Yuan, C.; Yu, H.; Zhang, G.; Qi, F.; et al. The Relationship between Particulate Matter Retention Capacity and Leaf Surface Micromorphology of Ten Tree Species in Hangzhou, China. *Sci. Total Environ.* **2021**, *771*, 144812. [CrossRef]
47. Zhang, W.; Zhang, Z.; Meng, H.; Zhang, T. How Does Leaf Surface Micromorphology of Different Trees Impact Their Ability to Capture Particulate Matter? *Forests* **2018**, *9*, 681. [CrossRef]
48. Zambrano, A.R.C.; Linis, V.C.; Nepacina, M.R.J.; Silvestre, M.L.T.; Foronda, J.R.F.; Janairo, J.I.B. Wetting Properties and Foliar Water Uptake of *Tillandsia* L. *Biotribology* **2019**, *19*, 100103. [CrossRef]
49. Amato-Lourenco, L.F.; Moreira, T.C.L.; de Oliveira Souza, V.C.; Barbosa, F.J.; Saiki, M.; Saldiva, P.H.N.; Mauad, T. The Influence of Atmospheric Particles on the Elemental Content of Vegetables in Urban Gardens of Sao Paulo, Brazil. *Environ. Pollut.* **2016**, *216*, 125–134. [CrossRef] [PubMed]
50. Martínez-Carrillo, M.A.; Solís, C.; Andrade, E.; Isaac-Olivé, K.; Rocha, M.; Murillo, G.; Beltrán-Hernández, R.I.; Lucho-Constantino, C.A. PIXE Analysis of Tillandsia Usneoides for Air Pollution Studies at an Industrial Zone in Central Mexico. *Microchem. J.* **2010**, *96*, 386–390. [CrossRef]
51. Pellegrini, E.; Lorenzini, G.; Loppi, S.; Nali, C. Evaluation of the Suitability of *Tillandsia usneoides* (L.) L. As Biomonitor of Airborne Elements in an Urban Area of Italy, Mediterranean Basin. *Atmos. Pollut. Res.* **2014**, *5*, 226–235. [CrossRef]

52. Vianna, N.A.; Gonçalves, D.; Brandão, F.; de Barros, R.P.; Filho, G.M.A.; Meire, R.O.; Torres, J.P.M.; Malm, O.; Júnior, A.D.; Andrade, L.R. Assessment of Heavy Metals in the Particulate Matter of Two Brazilian Metropolitan Areas by Using Tillandsia Usneoides as Atmospheric Biomonitor. *Environ. Sci. Pollut. Res.* **2011**, *18*, 416–427. [CrossRef]
53. Schreck, E.; Viers, J.; Blondet, I.; Auda, Y.; Macouin, M.; Zouiten, C.; Freydier, R.; Dufréchou, G.; Chmeleff, J.; Darrozes, J. Tillandsia Usneoides as Biomonitors of Trace Elements Contents in the Atmosphere of the Mining District of Cartagena-La Unión (Spain): New Insights for Element Transfer and Pollution Source Tracing. *Chemosphere* **2020**, *241*, 124955. [CrossRef]
54. Sun, X.; Li, P.; Zheng, G. Biomarker Responses of Spanish Moss Tillandsia Usneoides to Atmospheric Hg and Hormesis in This Species. *Front. Plant Sci.* **2021**, *12*, 50. [CrossRef]
55. Beringui, K.; Huamán De La Cruz, A.R.; Maia, L.F.P.G.; Gioda, A. Atmospheric Metal Biomonitoring Along a Highway Near Atlantic Rainforest Environmental Protection Areas in Southeastern Brazil. *Bull. Environ. Contam. Toxicol.* **2021**, *107*, 84–91. [CrossRef]